



HAL
open science

Turbulent flame propagation in large dust clouds

Christophe Proust

► **To cite this version:**

Christophe Proust. Turbulent flame propagation in large dust clouds. 11. International symposium on hazards, prevention, and mitigation of industrial explosions (ISHPMIE), Jul 2016, Dalian, China. ineris-01863026

HAL Id: ineris-01863026

<https://ineris.hal.science/ineris-01863026>

Submitted on 28 Aug 2018

HAL is a multi-disciplinary open access archive for the deposit and dissemination of scientific research documents, whether they are published or not. The documents may come from teaching and research institutions in France or abroad, or from public or private research centers.

L'archive ouverte pluridisciplinaire **HAL**, est destinée au dépôt et à la diffusion de documents scientifiques de niveau recherche, publiés ou non, émanant des établissements d'enseignement et de recherche français ou étrangers, des laboratoires publics ou privés.

Turbulent Flame Propagation in large Dust Clouds

Proust Christophe ^{a,b}

^a Institut de l'environnement industriel et des risques, PARC ALATA, BP2, Verneuil en Halatte, 60550, France

^b Sorbonne Universities, Technological University technologique of Compiègne, Escom, Centre Pierre Guillaumat, TIMR, bat E-D, Compiègne, 60200, France

E-mail : christophe.proust@ineris.fr

In order to be able to model correctly dust explosion propagation, data are needed to couple the flame velocity to the characteristics of the turbulence : intensity and scale. So far most of the available data were obtained with laboratory equipments. In this paper, large scale experiments (up to 100 m³) were performed during which both the flame velocity and turbulence characteristics were measured. Results are presented exhibiting a good correlation with the smaller scale data

Keywords: *dust explosions, flame propagation, turbulence*

1. Introduction

Since some decades, efforts have been made to develop numerical codes to try and help with the safe design of industrial facilities against explosions. A few are dedicated to dust explosions (Skjöld, 2007; Proust, 2005). One of the main challenges is to be able to correlate the local aerodynamics of the dust air mixture to the flame propagation. In particular, the incidence of the flow is targeted, since turbulence is always present in dust clouds. There is a need to find a correlation establishing the relationship between the combustion velocity (rate at which the mixture is burnt per unit flame area) and the characteristics of the turbulence.

Today, data are still severely lacking. Experiments are very difficult to do especially the measurement of the turbulence parameters. One of the pioneering works was performed 30 years ago, (Tezok et al., 1985). Experiments were done in a closed vessel and the turbulence intensity was measured during pretests without dusts with LDA or hot wire techniques, assuming it will be the same with the presence of dust particles and during flame propagation. Very often the flame speed is deduced and extrapolated from the pressure signals. Some progresses very made since that time and new data published (Krause and Kash, 2000; Sattar et al., 2014) but mostly at lab scale and with the same limitations.

During the last years however, evolutions were presented both in the way the measure the turbulence in the dust cloud in test conditions and to estimate the turbulent burning velocities both in closed bombs (Snoeys et al., 2006) and in the tube method (Schneider and Proust, 2007, Hamberger et al., 2007). But this is still the laboratory scale. In this paper, some estimations of the turbulent burning velocities of dust-air mixtures at larger scales are presented and compared to the small scale results.

Some basic turbulence and turbulent combustion are firstly recalled to point out the possible links between the main parameters. The experimental setups are presented and then the results and interpretation.

2. Turbulence and turbulent combustion

It was shown some time ago (Proust, 2006 a & b, Gao and al., 2015, Eckhoff, 1993) that the main lines of the explosion process may be very similar in gas and dust atmospheres. This is especially true for carbonaceous dust like flour, starch,... may be not for metal dusts.

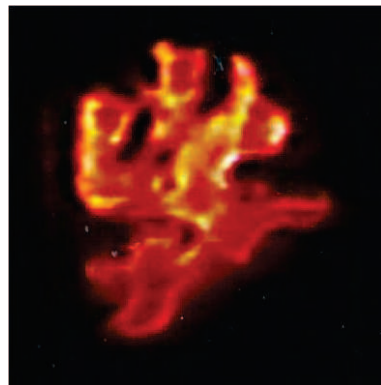
In particular, for those dusts burning in air, laminar, cellular and turbulent flame regimes were identified. The laminar flame regime obeys the same mechanisms: the reactants ahead of the combustion zone are heated by conduction up to being pyrolysed so that the combustion occurs in gaseous phase. Not surprisingly, the relevant parameters of this basic combustion regime are the consumption rate of the flame front, the “laminar burning velocity” S_1 , and the flame thickness, η_0 , deduced from S_1 using the thermal diffusivity of the medium.

A flow becomes turbulent as soon as, inside a boundary layer (velocity gradient), the low speed layers of the flow are rolling up with the higher speed layers to produce eddies which appear and dissipate rapidly. Such structures are “chaotic” and can be studied using statistics which has been done for nearly one century : these structures constitute the “turbulence” of the flow (Hinze, 1975). The relevant theories introduce the notion of “turbulent cascade” according to which the initial eddies are destroyed in smaller and smaller structures until dissipation by molecular diffusion so that there is a mechanical link between all the structures of the turbulence. In practice, this “cascading” process is seen as an intrinsic process, independent from the mean flow. Because of this, it is then sufficient to know the characteristics of the largest eddies, those directly issued from the average flowfield, to fully characterize the turbulence. These characteristics are the scale of the largest eddies (L = “integral scale of turbulence”) and their peripheral velocity (u' = “rms of the velocity fluctuations”). The parameter u' is in principle a space averaged variable and L is the area under the curve giving the evolution of the correlation coefficient of the velocity signals around a reference point.

It is implicitly assumed that the situation may be comparable with dust clouds (Tezok et al., 1985). This is not fully obvious however, since for instance, direct observation show that the particles are pushed around the turbulent eddies (Proust, 2006b, Bozier, 2004). The mixture does not remain locally homogeneous, and as a consequence, the burning may occur mostly at the periphery of the eddies and potentially in between (figure 1). This makes a difference with turbulent burning in homogeneous gaseous flames. To our knowledge, this issue has not been addressed yet.



Turbulent cloud (laser tomo.)



Turbulent flame

Fig. 1. Visual aspect of a turbulent flow of starch dust air mixture and of turbulent flame propagating in that cloud (scale = 10 cm wide tube)

So the turbulent flame propagation in premixed gaseous mixtures remains the model to refer to. Unfortunately, the propagation mechanisms are still a matter of passionate debate and are the subject of active research. For the present purpose, it is sufficient to recall that the parameter of interest is the “turbulent burning velocity”, S_t , defined in a somewhat similar way as the laminar burning velocity. It can be viewed as the local flame consumption rate over the averaged flame front and should represent the speed at which the flame progresses against the mean flow. For those situations where the turbulent flame can be seen as a disturbed version of a laminar flame, which should be the case when $L \gg \eta_0$ (Borghi and Destriau, 1998), the characteristics of the turbulence should be coupled to those of the laminar flame front in the propagation process. Following S_t should be a function of S_l , η_0 , u' and L . A number of approaches, sometimes conceptually diverging, were used to derive such a relationship over time (Bray, 1990; Gülder, 1990; Yakhot, Peters, 1986) but a simple engineering dimensional analysis says that the relationship should be :

$$\frac{S_t}{S_l} = K \cdot \left(\frac{u'}{S_l} \right)^\alpha \cdot \left(\frac{L}{\eta_0} \right)^\beta$$

Where K , α and β are constants. A tentative use of the Gülder model ($K=0.6$, $\alpha=0.75$, $\beta=0.25$), resembling also that proposed by Peters, was proposed (Schneider and Proust, 2005, Hamberger and al., 2007) and seems to correlate well with lab scale experiments (Figure 2 : $L=0.03$ m). Noteworthy the characteristics of the turbulence were measured in the dust cloud using a technique very similar to that explained hereafter.

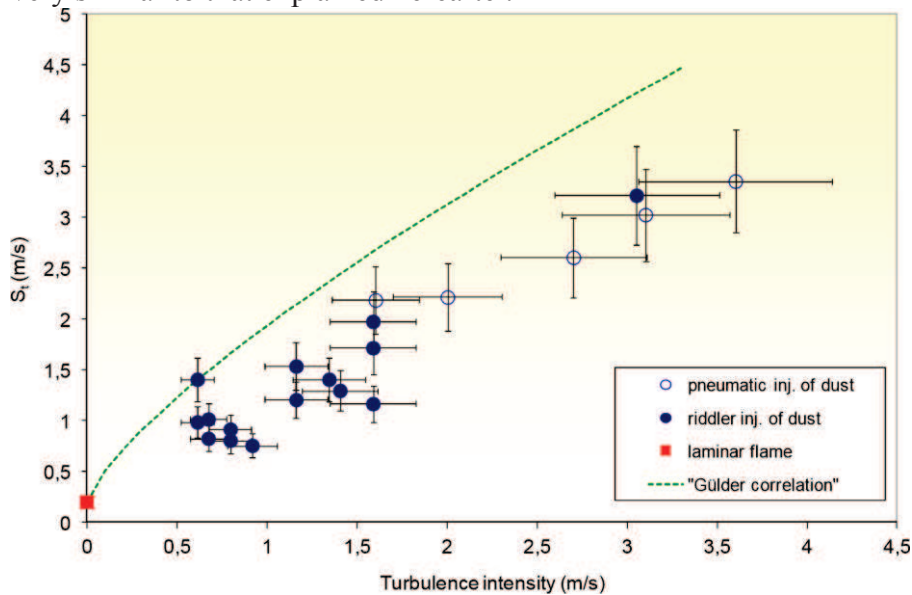


Fig. 2. Turbulent starch (*Microlys* and *Swely gel*) dust air flames propagating in a tube ($L=0.03$ m; u' between 1 and 4 m/s from Schneider and Proust, 2007) with a dust concentration between 500 and 1000 g/m^3 .

The agreement seems very reasonable but there is a need to verify it further especially in view of capturing the scale effect. To this purpose large scale experiments were performed.

3. Setups and metrology

3.1 Chambers

Experiments were done using a 1 m^3 closed vessel, a 10 m^3 vessel and a 100 m^3 chamber (figure 3).

Table 1: main characteristics of the explosion chambers.

Chamber (L/D)	Ignition point	Ignition source	Dust dispersion	Vented
1 m ³ (1.7)	Center	2 x 5 kJ igniters	5 l – 20 bar bottle and perforated ring	closed
10 m ³ (3.7)	Opposite to dispersion	50 kJ flash powder	Pressurized dust nozzle	0.5 m ²
100 m ³ (3.3)	Closed end	50 kJ flash powder	Pressurized dust nozzle	3, 6, 8 m ²



Perforated ring of the 1 m³ vessel



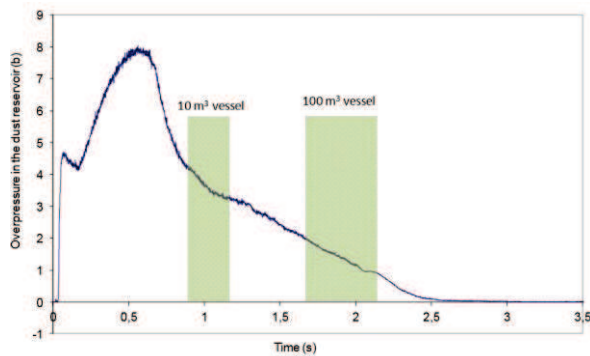
1 m³



10 m³



100 m³



Overpressure in the pressurized dust nozzle



Pressurized dust nozzle (other chambers)



Dust dispersers in the 100 m³ vessel

Fig. 3. *Various details about the explosion chambers*

In the 1 m³ vessel the dispersion system is that described in the international ISO 6184/1 standard. The dust is contained in a 5 l reservoir pressurized up to 20 bar (air). An electrical or pyrotechnical valve releases the dust in the chamber via a perforated ring. The overall release area is about 300 mm². The ignition source is normally activated about 600 ms after the start of the dust dispersion. But in the frame of the present testing a larger ignition delay was used (1500 ms) in some instances to obtain a lower level of turbulence. Also, an additional bottle of pressurized air was added for some tests to increase the turbulence level (keeping the 600 ms ignition delay which is required to empty the dust reservoir : Snoeys et al., 2006).

For the other chambers a powerful pneumatic dust disperser was systematically used. It is made of a circular 32 mm orifice (1200 mm² release area) connected to a curved reservoir (150 mm internal diameter; 700 mm long). To trigger the dispersion, pressurized air is injected at the top of the reservoir so that the pressure jumps at about 7 bar (gauge) at the early beginning of the discharge process and drop to zero in about 2 seconds.

Only one disperser was used in the 10 m³ vessel and was located on an end flange opposite to the ignition source (on the other end flange). The ignition source is located on the axis of the chamber at 0.8 m from the flange and the ignition delay (elapsed since the pressurization of the disperser) is about 800 ms.

Up to 4 dust dispersers were installed in the 100 m³ vessels on the frame middle in the chamber (at 5 m from the blind end). The ignition source was located in the center of the rear wall, opposite to the vented section and the ignition delay (elapsed since the pressurization of the disperser) is about 1700 ms.

3.2 Measurements

3.2.1 Pressure, temperature and flame detection

The overpressure are measured classically Kistler Piezoresistive (0-10 bar) transducers. One is mounted flush on the outer wall of the chamber (in the middle between both extremities) and is

thermally insulated. The second one is mounted on the dust reservoir to control the discharge.

In some cases, K thermocouples (1 mm) were used (with the 1 m³ vessel exclusively).

The detection of a propagating flame can be a challenge especially when short distances are concerned (Snoeys et al., 2006). Usually optical detectors can be employed when separations distances are a meter at least. Amplified photodiodes were used with the 100 m³ chamber. With shorter run up distances, ionization gages can be used. These were employed with the smallest devices. The electrodes (4 to 6) were aligned on a rod of 0.5 m long close to the ignition source, where the flame is expected to grow isotropically so that the flame velocity is the expansion velocity (expression (2)).

3.2.2 Turbulence

One of the greatest difficulties is to be capable of measuring the turbulence in a dust air mixture. Standard laboratory equipments and especially LDA and hot wire anemometry are not applicable. INERIS has been working for years on the development of alternative techniques (Proust, 2004). A Pitot tube technique based on a very refined concept of Mc Caffrey gauges (Mc Caffrey, 1976) was implemented (Fig. 4). The device provides results fully in line with traditional techniques (in figure 4 the turbulence measured in the 1 m³ ISO vessel is shown and compared to LDA measurements : from Snoeys et al., 2006). It was used to do the measurement of figure 2. The sensor head is a short tube (length 2 cm , diameter 1 cm) with a solid wall in the middle and the differential pressure is measured on both sides with a precise and fast pressure transducer. The aeraulics of the system had to be refined to have sufficient dynamics. Extensive testing in a reference jet proved that such transducers are able to detect eddies as small as 2 cm with a peripheral velocity of 0.2 m/s. Note in particular that the devices can do measurements even in very dusty mixtures (up to 500 g/m³ at least).

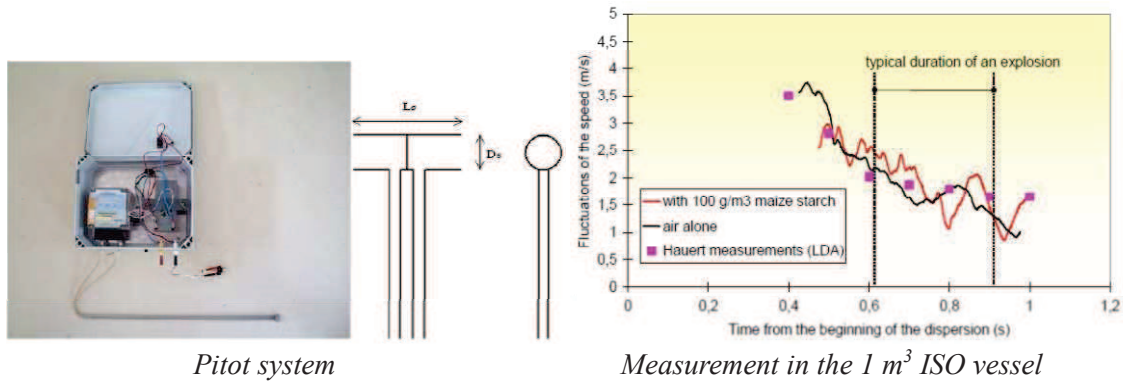


Fig. 3. Turbulence measurement device and examples of arrangement

Most turbulence measurements were obtained without dust being dispersed in the chambers but some were performed with dust and gave similar results (Snoeys et al., 2006).

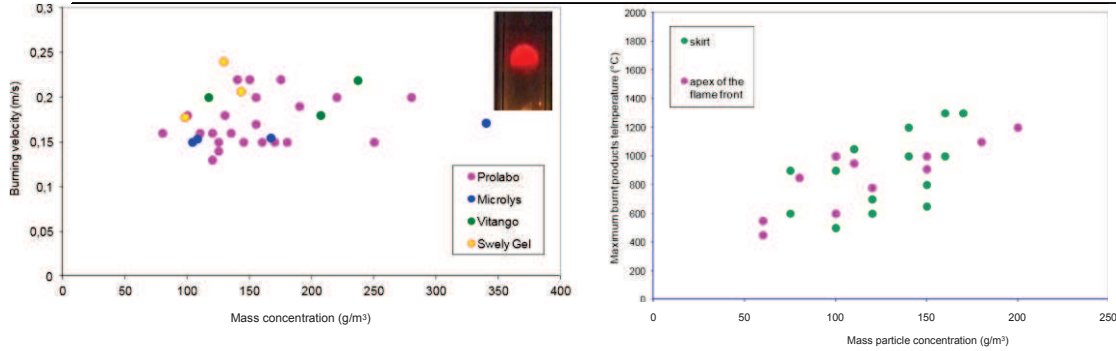
3.3 Results

3.3.1 Combustible mixtures

The results presented hereafter were obtained with starch based dusts because the laminar burning velocities and burnt products temperatures are known (Proust, 2006a; Schneider and Proust, 2007). Some published data are recalled below about the fundamental burning properties (measurements using the tube method – 10 cm diameter and 25 μm diameter K thermocouples for the temperature measurements).

Table 2: main combustion properties of some starches.

Reference	Sauter mean dia. (μm)	Laminar burning velocity (m/s at 250 g/m^3)
Prolabo (Proust, 2006b)	34	0.20 ± 0.05
Microlys (Schneider and Proust, 2005)	14	0.16 ± 0.02
Vitango (Schneider and Proust, 2005)	25	0.20 ± 0.03
Swely gel (Schneider and Proust, 2005)	16	0.22 ± 0.03 (150 g/m^3)



Laminar burning velocities

Maximum burnt products temperatures

Fig. 4. Fundamental burning properties of starch dust-air mixtures

There is no discernable influence of the nature of the starch and of the particle size. It may then be estimated that the above parameters are representative of the agricultural dusts used for the present testing (table 3).

Table 3: dusts used for the large scale experiments (present paper).

Reference	Sauter dia. (μm)	Concentration (g/m^3)	Max. expl. Overp. (b)	Kst (b.m/s)
Wheat flour (bakery)	47	250 and 500	7.3	70
Corn starch	13	250 and 500	7.3	100

A limited number of comparative tests were done using stoichiometric methane-air mixtures (1 m^3 vessel).

3.3.2 Flowfield

Several of the turbulence probes have to be used simultaneously to do a measurement because first the turbulence may not be homogeneous and second because the signals have to be cross correlated to derive the integral scale of the turbulence (see Schneider and Proust, 2007 for further details). A typical example of such a display is shown on figure 5 for the specific case of the 1 m^3 vessel. Apart in the jet region, there is no average flow inside the vessel but mostly turbulence at least in the combustion time slot. In this particular case, the turbulence probes were too close not to disturb the largest structures of the turbulence and an alternative method was employed to estimate the integral scale of the turbulence. The probes were separated and their signal was correlated in time during the period where a measurable average velocity was detected. The autocorrelation time multiplied by this velocity gives an image of the space correlation (Taylor assumption). The results are presented in figure 4 showing the space correlation obtained this way and the cross correlation of the probes. Clearly, the probes tend to be strongly correlated suggesting there are in the same region of the flow but also that they interact and influence each of them. So the integral scale of the turbulence is about 3 to 4 cm

whereas the intensities of the turbulence are respectively 1.7 m/s in the standard conditions, 0.7 m/s when the ignition time is 1500 ms and 4 m/s in the reinforced turbulence configuration.

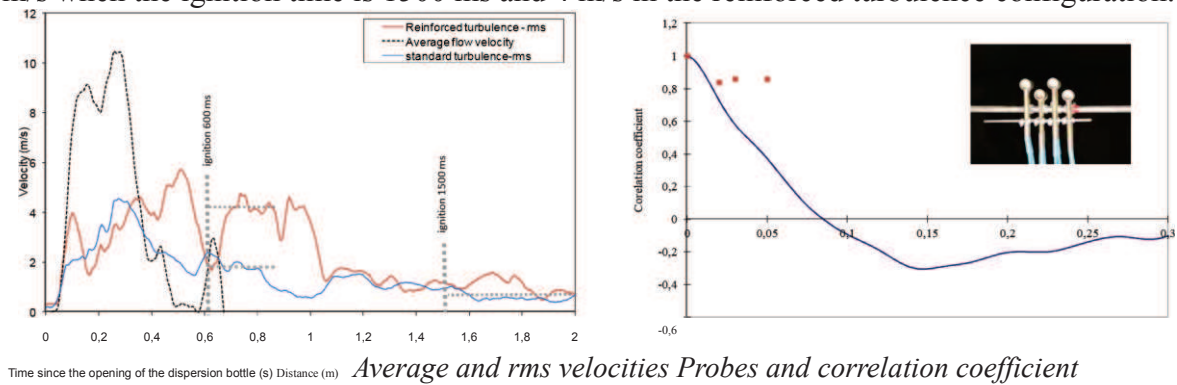


Fig. 5. Turbulence probes arrangement and results (1 m^3 vessel)

A set of vertically aligned turbulence probes was installed in the geometrical centre of the 10 m^3 chamber. The results are presented on figure 6. As for the “elongated” 1 m^3 vessel, there is an average axial velocity of about 2 m/s but is much less. The turbulence intensity is about 3 m/s and the integral scale of turbulence is about 5 to 10 cm with a reasonable agreement between the time and space correlations.

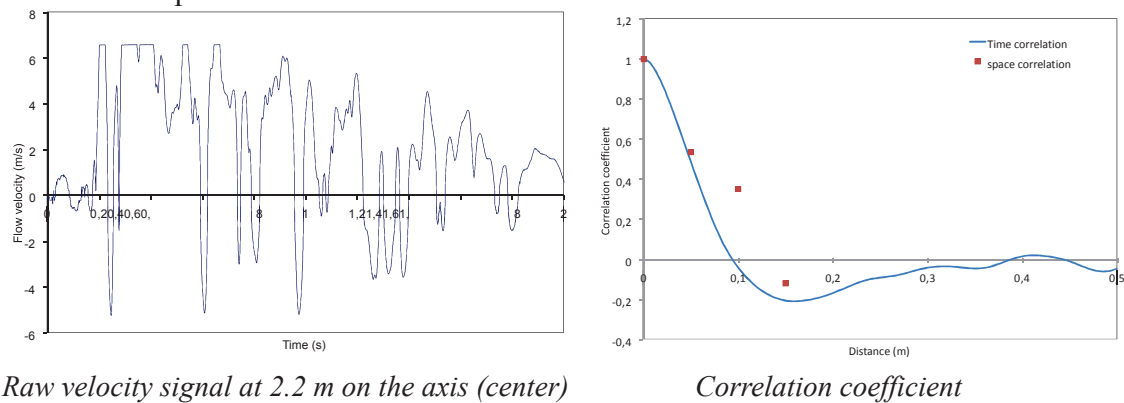


Fig. 6. Turbulence results (10 m^3 vessel)

Similarly, a set of vertically aligned turbulence probes was installed on the axis of the 100 m^3 chamber and moved between the blind end towards the vented end. The results are presented on figure 7. The average flow velocity is about 0 m/s and the rms of the fluctuations (u') is not far from 1 m/s at least in the ignition zone. From the area, under the curve of the spatial cross correlation coefficient the integral scale of the turbulence can be deduced and is about 20 cm.

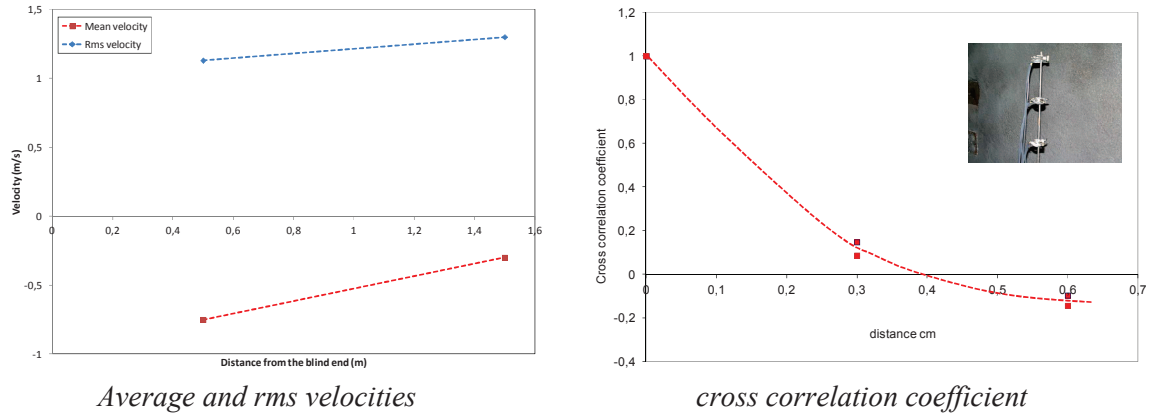


Fig. 7. Turbulence results (100 m^3 vessel)

The turbulence characteristics are gathered in table 4. Clearly the measurements obtained with the 1 m^3 vessel fall in the range of the laboratory scale experiments and should give similar results in terms of turbulent burning velocities. A significant scale up effect is possible only with the largest equipment.

Table 4: turbulence characteristics of the various setups.

Nature	Turb. Intensity (m/s)	Int. lengthscale (m)
30 cm tube (Schneider and Proust)	0.5 to 4	0.03
1 m^3 chamber	0.7 to 4	0.04
10 m^3 chamber	3	0.07
100 m^3 chamber	1	0.2

3.3.3 Explosion overpressures and burnt product temperatures

Theoretically there is a link between the adiabatic combustion temperature at constant pressure and the adiabatic combustion temperature at constant volume. For the same reactants and quantities, the same amount of energy is released. So :

$$N_{\text{products}} \cdot C_p \cdot (T_{p\text{max}} - T_{\text{init}}) \approx N_{\text{products}} \cdot C_v \cdot (T_{v\text{max}} - T_{\text{init}}) \quad (1)$$

Where C_p and C_v are the specific molar heat capacities of the burnt products at constant pressure and volume, N_{products} the number of moles of products, $T_{p\text{max}}$ and $T_{v\text{max}}$ respectively the maximum burnt products temperatures at constant pressure and volume (T_{init} , the initial temperature). Assuming all is gaseous in the products, using the equation of state (perfect gas law) and knowing that $C_p = \frac{\gamma_p \cdot R}{\gamma_p - 1}$ and $C_v = \frac{R}{\gamma_p - 1}$ (R the perfect gas constant and γ_p the ratio of the specific heats at T_{max} , typically 1.3) :

$$\gamma_p \cdot (E - 1) \approx \frac{P_{v\text{max}}}{P_{\text{init}}} - 1 \quad (2)$$

where E stands for the volumetric expansion ratio of the burnt products and P_{max} the adiabatic explosion pressure at constant volume. Note that we may also derive from (1):

$$\gamma_p \cdot \left(\frac{T_{p\text{max}}}{T_{\text{init}}} - 1 \right) \approx \frac{T_{v\text{max}}}{T_{\text{init}}} - 1 \quad (3)$$

If N_{init} is the initial number of moles :

$$E = \frac{N_{products} \cdot T_{pmax}}{N_{init} \cdot T_{init}} \quad (4)$$

E would be close to T_{pmax}/T_{init} only if $N_{product}/N_{init}$. There is a possibility to derive $N_{products}/N_{init}$ from the measurement of T_{vmax} and P_{max} using the perfect gas law to rewrite the right hand side of expression (1):

$$\frac{P_{vmax}}{P_{init}} = \frac{N_{products}}{N_{init}} \cdot \frac{T_{vmax}}{T_{init}} \quad (5)$$

The measurements of T_{vmax} and P_{vmax} were measured in the 1 m³ vessel (figure 8).

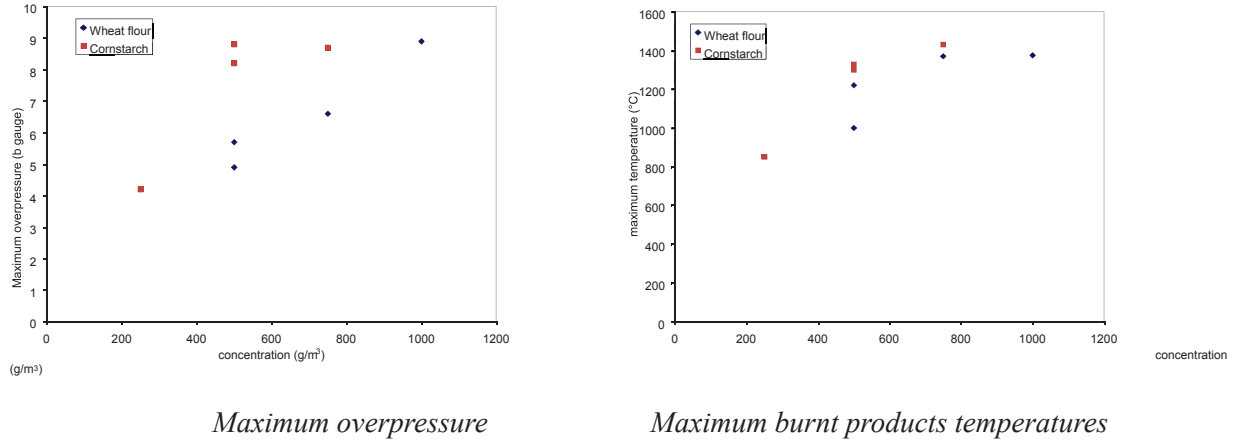


Fig. 8. Maximum explosion overpressures and temperatures measured in the 1 m³ vessels (cornstarch and wheat flour).

Knowing that T_{vmax}/T_{init} is about 5.7 at maximum, it can easily be shown, using expression (3), that T_{pmax}/T_{init} should be on the order of 4.7 so that $T_{pmax} = 1100^{\circ}\text{C}$ which is fully in line with the data from figure 4.

The expansion ratio, deduced from equation (2) and the relationship (5) are represented on figure 9.

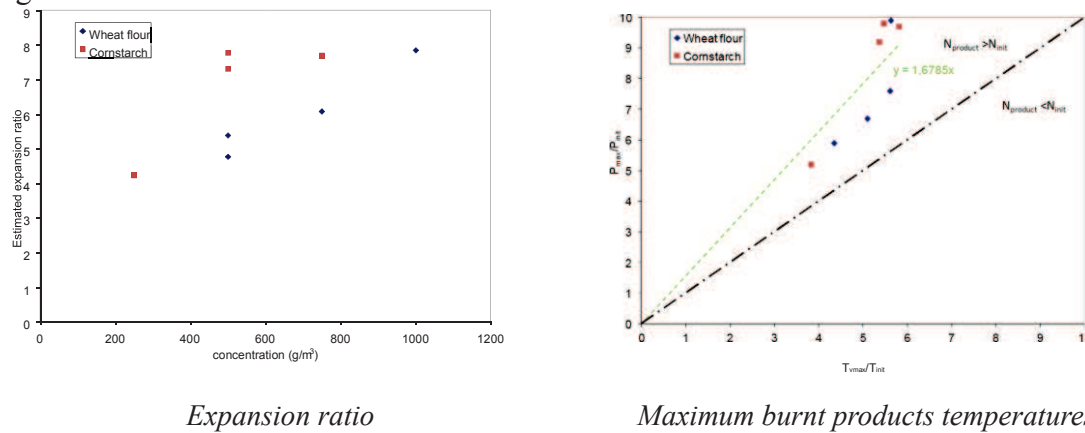


Fig. 9. Estimation of the expansion ratio and of $N_{products}/N_{init}$ from the data of figure 9.

The expansion ratio is clearly greater than the ratio T_{pmax}/T_{init} (maximum 5) so that expression [4] suggests $N_{product}/N_{init}$ should be significantly greater than 1. On average this ratio is about 1.7. The reason for this could be that, in most experimental situations, the concentration of dust is well above the stoichiometric conditions (250 g/m³) so that the excess dust can be pyrolysed in the very hot burnt products (starch gasify at 400°C in flames : Proust 2006b) producing a significant amount of gases. This point was suggested earlier (Lemos, xxx).

For the purpose of the present investigation, with mass particle concentrations ranging between 250 and 500 g/m³, an average value of 5 was chosen for E.

3.3.4 Flame dynamics

Careful velocity measurements were carried out especially in the 1 m³ vessels (Snoeys et al., 20086) using ionization gages (figure 10). Five of them were installed along the axis of the chamber, the ignition source being close to the first one. Ionization probes detect the combustion zone of the flame and are much more accurate than photodetectors over short separation distances. On that particular example, S_f=6 m/s.

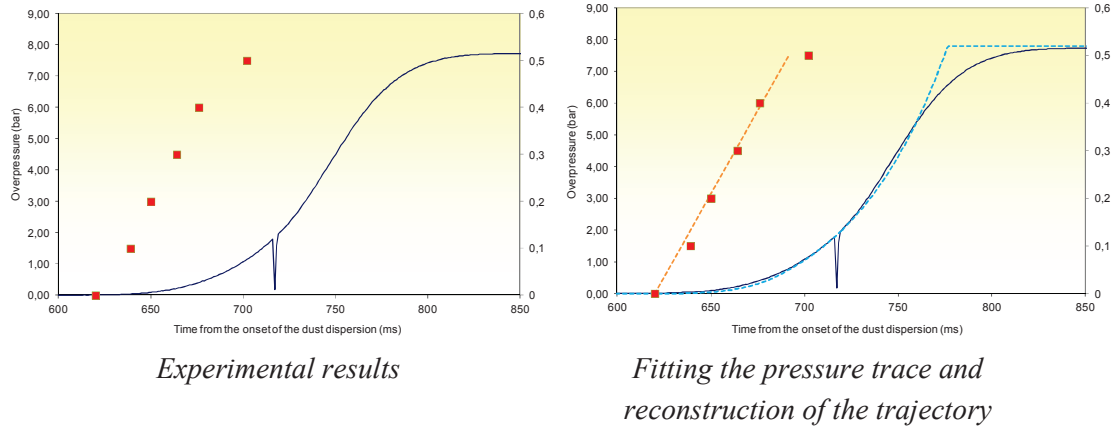


Fig. 10. Flame trajectory and pressure trace in the “cubic” 1 m³ chamber (500 g/m³ cornstarch, standard dust dispersion procedure).

Note that the measured spatial flame velocity S_f is not S_t. If E stands for the expansion ratio of the burnt products, the relationship would be :

$$S_f = S_t \cdot E \quad (6)$$

at least at the beginning of the propagation of the flame when the compression effect is low (typically whenever the volume of the burnt products is less than 20% of the vessel volume). In the vessels, the ionisation gages follow the flame trajectory along the first 40 to 50 cm which is well inside this limit. A good estimation of S_t may be obtained if the expansion ratio would be known. As chosen above, E is on the order of 5. S_t is then about 1.3 m/s for the example of figure 10.

It would be interesting to make a link with the pressure trace. A route was proposed in a earlier work (Snoeys et al., 2008). Assuming that the compression is adiabatic, it can be established that :

$$\frac{dP}{P \cdot dt} = \frac{\gamma}{V} \cdot S_f \cdot A_f \cdot (E - 1) \quad (7)$$

Where P is the internal pressure, and A_f the flame area at time t and γ an average value for the ratio of the specific heats (typically 1.35). Reasonable assumption can be made such that the flame ball develops approximately spherically around the ignition source until reaching the outer walls. After, and possibly for some limited amount of time the flame front will propagated as two hemispherical caps until meeting with the end flanges. When this approximation is used together with the estimated values of E, it is possible to choose S_t so that the calculated pressure trace matches the best with the measured pressure trace. The flame trajectory can then be reconstructed.

This second method provided results very close from the former. This kind of analysis provides a means to derive a burning velocity from a pressure trace when the flame trajectory is lacking or too partial.

This treatment was applied to the 100 m³ experiments (Figure 11) for which measurements of the flame trajectory are available (photodetectors). The flame folding factor was chosen constant and equal to 4 after the flame front has reached the outer walls (the initial flame propagation phase up the lateral wall is assumed to be roughly hemispherical). With this assumption the best fit is obtained between the pressure traces and the trajectory of the leading edge of the flame front. The fit is not as good because the flame folding factor is not constant. The flame elongates progressively in the direction of the vent. On the basis of the geometry the largest flame folding factor should be about 6. 4 is certainly a reasonable estimate.

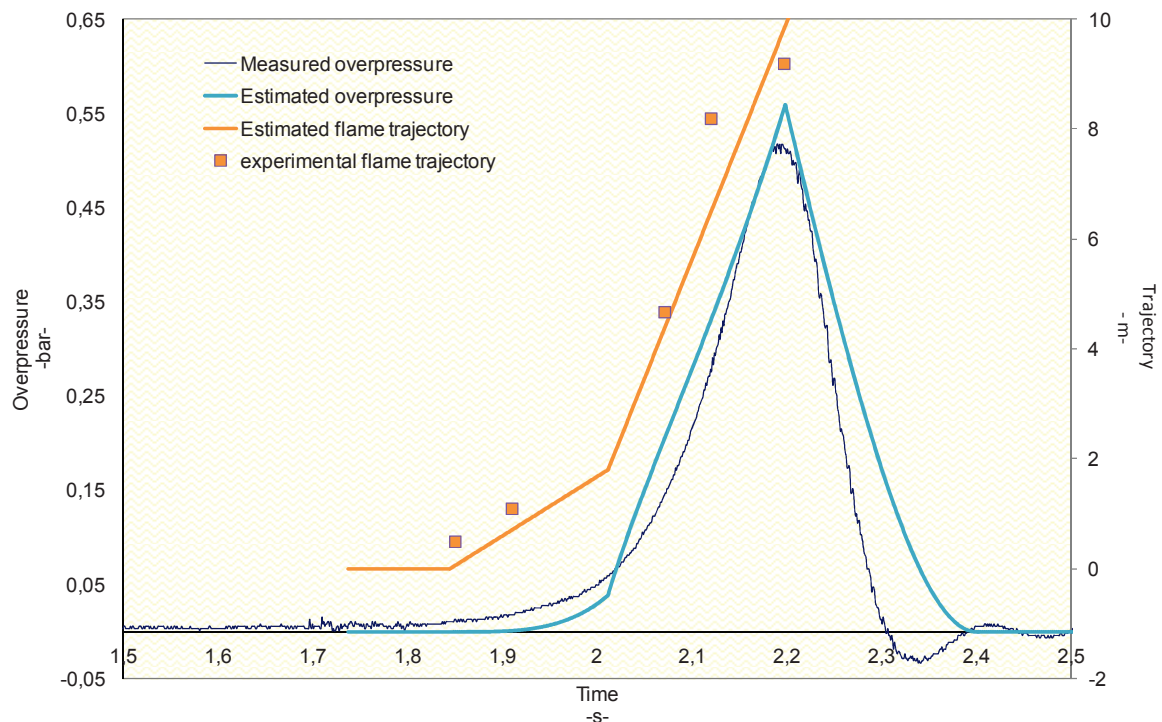


Fig. 11. Flame trajectory and pressure trace in the 100 m³ chamber (250 g/m³ cornstarch, vent area 3 m²).

The same technique was used for the 10 m³ vessel (with the same flame folding factor), for which only very limited information is available (figure 11), and a good agreement is reached. In this case S_t is about 2 m/s.

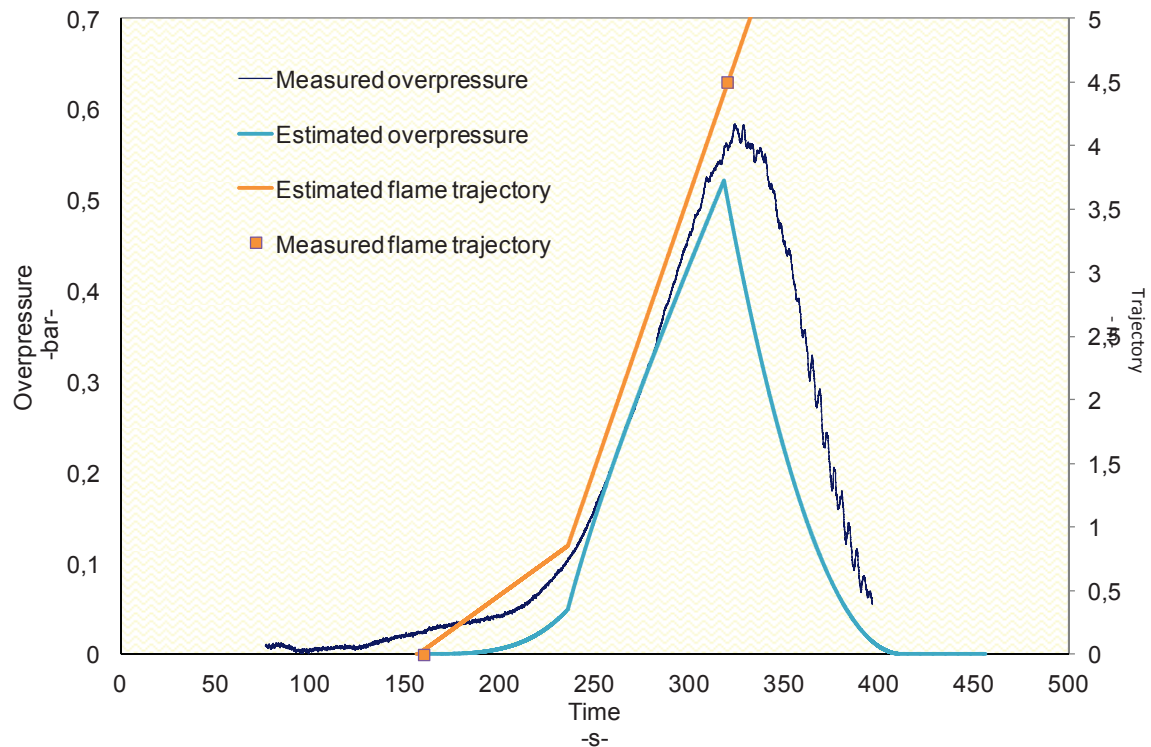


Fig. 12. Flame trajectory and pressure trace in the 10 m³ chamber (250 g/m³ cornstarch, vent area 0.5 m²).

3.3.5 Turbulent velocity data

Using the methods and tools described above, the turbulent burning velocities of cornstarch and wheat flour were extracted. The data are presented in table 5.

Table 5: turbulent burning velocities extracted from 1, 10 and 100 m³ experiments (accuracy $\pm 20\%$)

Description	u' (m/s)	Lt (m)	St (m/s)
1 m ³ chamber – wheat flour – 500 g/m ³	1	0.04	0.4
1 m ³ chamber – wheat flour – 500 g/m ³	1.5	0.04	0.7
1 m ³ chamber – cornstarch – 250 g/m ³	1.7	0.04	1.2
1 m ³ chamber – cornstarch – 500 g/m ³	1.7	0.04	2.4
1 m ³ chamber – cornstarch – 250 g/m ³	4	0.04	2.4
1 m ³ chamber – cornstarch – 500 g/m ³	4	0.04	3.0
1 m ³ chamber – cornstarch – 250 g/m ³	0.7	0.04	0.4
1 m ³ chamber – cornstarch – 500 g/m ³	0.7	0.04	0.5
10 m ³ chamber – wheat flour – 250 g/m ³	3	0.07	2
100 m ³ chamber – wheat flour – 300 g/m ³	1	0.2	2
100 m ³ chamber – wheat flour – 500 g/m ³	1	0.2	2.4
100 m ³ chamber – wheat flour – 500 g/m ³	1	0.2	3.1

It is interesting to compare this additional information with the results obtained at a smaller scale (figure 13). Both set of data compare relatively well. This can be justified considering the chemical similarities of the dusts and of the integral scales of turbulence. Wheat flour data

seem to be slightly below and may be in line with the fact that the reactivity of wheat flour seems lower (table 3).

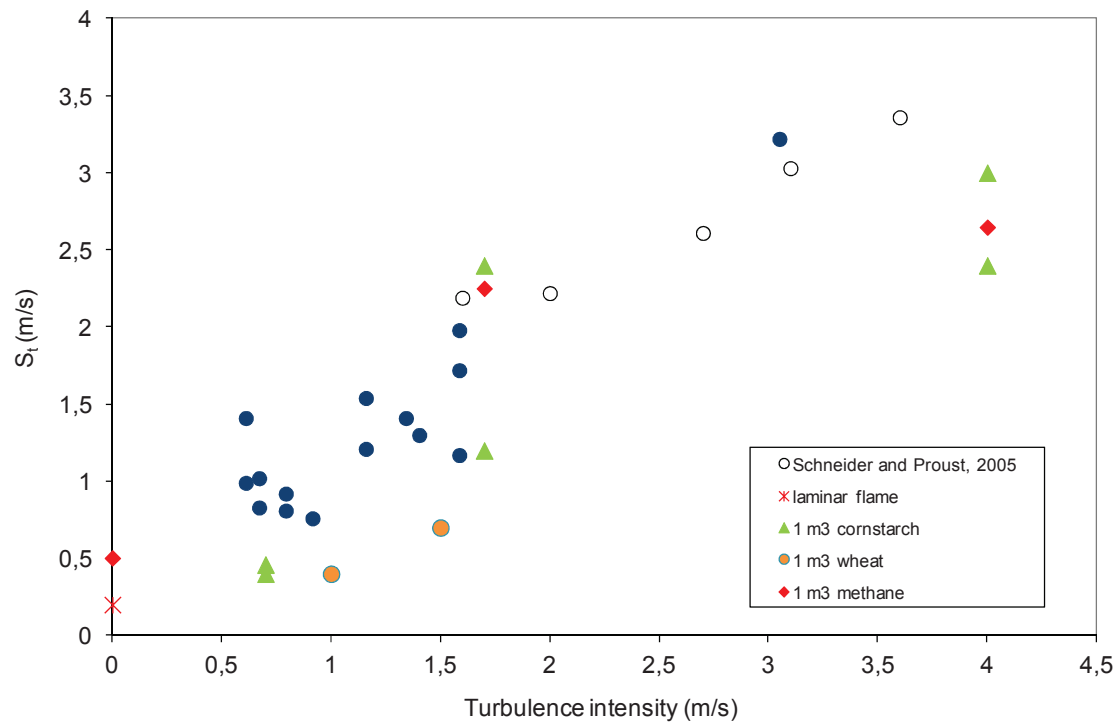


Fig. 13. Comparison of the S_t - u' correlation between the laboratory scale results and the 1 m³ experimental results

In the same conditions, stoichiometric methane-air explosions were produced and seem also in line with the dust data although somewhat higher. Similarly this would result from the larger laminar burning velocity of methane-air mixtures (0.3 to 0.4 m/s as compared to 0.2 m/s).

Larger scale experimental results are shown on figure 14. The 10 m³ vessel experiments seem to fit with the 1 m³ data. The integral length scale measured in the 10 m³ vessel is close to that obtained in the 1 m³ which might justify this behaviour. Nevertheless, the large scale experiments were obtained with wheat flour, less reactive than starch. Considering this, a scale effect may be discernible about the 10 m³ vessel, which is even clearer with the 100 m³ experiments.

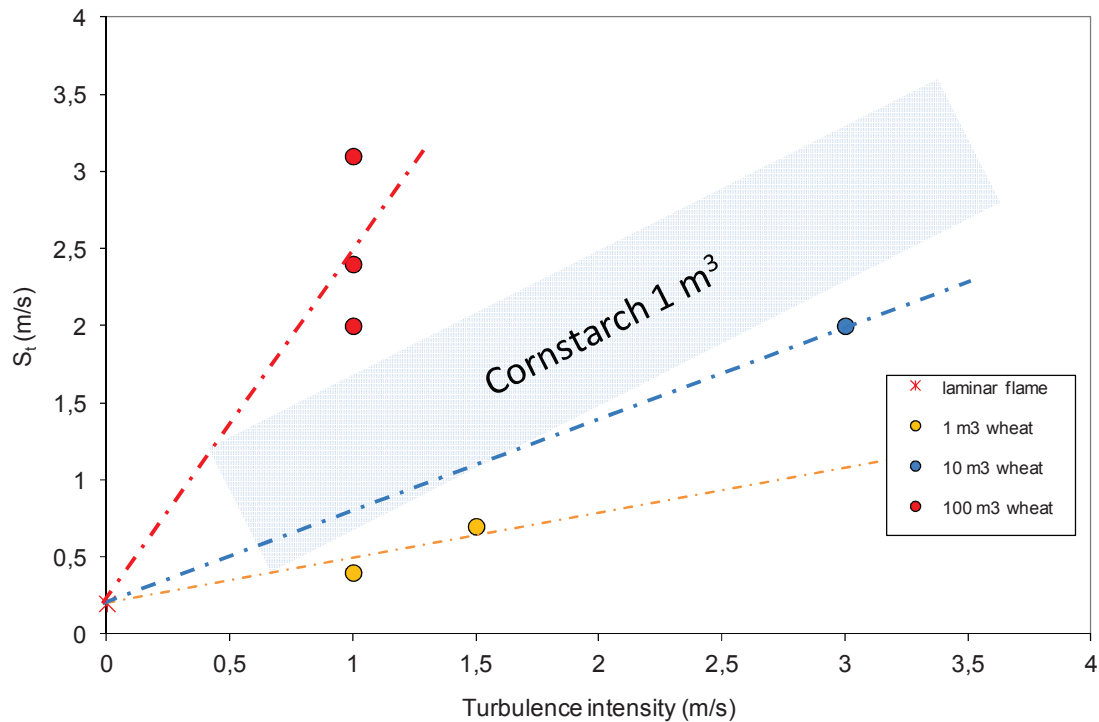


Fig. 14. S_t - u' relationship as function of the scale of the experiments

4. Conclusion and perspectives

This paper is intended as a contribution to correlating turbulence and turbulent flame propagation in dust air mixtures. Setups, metrology and methods to analyze the data are first presented including flame dynamics considerations.

Results are presented for starches incorporating laboratory scale setups to large scale explosion chambers (100 m³). Laboratory results once suggested that the Gülder model developed for gaseous mixtures might be applicable to dust air mixtures as well (Schneider and Proust, 2007, Hamberger and al., 2007).

If it were so, the turbulent burning velocity would scale as $L_t^{0.25}$ where L_t is the integral scale of the turbulence. Data from figure 14, suggest a L_t dependency which is first order dependency.

Although much more data are certainly required to verify this, the reader should be aware of the intrinsic differences between a turbulent dust cloud and a turbulent gaseous mixture. The latter remain chemically homogeneous whereas in the former the centre of the eddies is deprived from particles. This certainly strongly affects the burning mechanism which, in particular, could not fit with the assumptions used by Gülder to establish his model. So a closer look into the turbulent combustion mechanisms is certainly required also.

References

- Bray K. (1990). Studies of turbulent burning velocities, Proceedings of the Royal Society of London, vol. A431, pp. 315-325
- Bozier O., Veysière B. (2006), Influence of suspension generation on dust explosion parameters, Combustion Science and Technology, vol. 178, no. 10-11, pp. 1927-1955
- Eckhoff, R.K. (2003). *Dust explosions in the process industries*. Third edition. Gulf Professional Publishing, Amsterdam.
- Gao W., Mogi T., Yu J., Yan X., Sun J., Dobashi R. (2015), Flame propagation mechanisms in dust explosions, Journal of Loss Prevention in the Process Industries, <http://dx.doi.org/10.1016/j.jlp.2014.12.021>
- Gülder Ö.L. (1990). Turbulent premixed flame propagation models for different combustion regimes, Comptes-rendus du 22nd Symp (Int.) on Combustion
- Hamberger, P., Schneider, H., Jamois, D., Proust, C. (2007), Correlation of turbulent burning velocity and turbulence intensity for starch dust air mixtures, Third European Combustion Meeting (ECM2007), in Chania, (Crete)
- Hinze J.O. (1975). Turbulence, 2nd edition, Mc Graw-Hill company, New-York, ISBN 0-07-029037-7
- Krause U., Kasch T. (2000), The influence of flow and turbulence on flame propagation through dust-air mixtures, Journal of Loss Prevention in the Process Industries, vol. 13, 291–298
- Lemos L., Bourianne R. (1989), Starch dust combustion characteristics in a closed spherical vessel, 12th ICDERS, Ann Arbor, USA
- Mc Caffrey, B.J. & Heskestad, G. (1976). A robust bidirectional low-velocity probe for flame and fire application, Comb. and Flame, 26, 125.
- Peters N. (1986), "Laminar flamelet concepts in turbulent flames", Comptes-rendus du 21st Symp. (Int.) on Comb., The Combustion Institute
- Proust Ch. (2004), « Formation, inflammation, combustion des atmosphères explosives (ATEX) et effets associés », Mémoire d'HdR présenté à l'Institut National Polytechnique de Lorraine, 12 Fév 2004
- Proust Ch. (1999). Mécanismes de dispersion et d'explosion lors de fuites d'hydrogène liquide, Rapport final d'une étude réalisée pour le Ministère de l'Environnement, ref 11AP50
- Proust, Ch. (2005). The usefulness of phenomenological tools to simulate the consequences of dust explosions : the experience of EFFEX, Presented at the ESMG meeting, Nürnberg, 11-14 oct 2005
- Proust, Ch. (2006a). Flame propagation and combustion in some dust air mixtures, J. Loss Prev. Process Ind., vol. 19, pp. 89-100
- Proust, Ch. (2006b), A few fundamental aspects about ignition and flame propagation in dust clouds, J. Loss Prev. Process Ind., in press.
- Sattar H., Andrews G.E., Phylaktou, H.N., Gibbs B.M. (2014), Turbulent flame speeds and laminar burning velocities of dust using the ISO 1 m³ dust explosion method, Chemical Engineering Transactions, Vol. 36
- Schneider, H. and Proust, Ch. (2005). Laminar and Turbulent Burning Velocities of Dust Clouds. International ESMG Symposium on Process Safety and Industrial Explosion Protection, Nürnberg, Germany

- Schneider, H., Proust, C. (2007), Determination of the turbulent burning velocities of dust air mixtures with the open tube method, *Journal of Loss Prevention in the Process Industries*, vol. 20: 470-476
- Skjöld T. (2007), Review of the DESC project, *Journal of Loss Prevention in the Process Industries* 20 (2007) 291–302
- Snoeys J., Proust C., Going J. (2006), Experimental studies of turbulent flame speeds, 6th ISHPMIE, Halifax, Canada, August 2006
- Tezok, F.I., Kauffman, C.W., Sichel, M., & Nicholls, J.A. (1985). Turbulent Burning Velocity Measurement for Dust/Air Mixtures in a Constant Volume Spherical Bomb. 10th ICDERS, Berkeley.
- Yakhot V. (1988), Propagation Velocity of Premixed Turbulent Flames, *Combustion Science and Technology*, Volume 60, Issue 1-3, pp 191-214